Sedimentologika

10.57035/journals/sdk.2026.e41.1927

Along-strike variability of fault-controlled deltaic systems (Crati Basin, southern Italy)

Candela Martínez* [1,2], **Christopher A.-L Jackson** [3], **Nicola Scarselli** [1], **Sergio G. Longhitano** [4], **Francesco Muto**[5], **and Domenico Chiarella** [1,6]

[1]Clastic Sedimentology Investigation (CSI), Department of Earth Sciences, Royal Holloway University of London, London, TW20 0EX, UK
[2]Department of Analytic Sciences, Universidad Nacional de Educación a Distancia, Madrid, 28015, Spain
[3]Department of Earth Science and Engineering, Imperial College London, London, SW7 2BX, UK
[4]Department of Basic and Applied Sciences, Università della Basilicata, Potenza, 85100, Italy
[5]Department of Biology, Ecology and Earth Sciences, University of Calabria, Cosenza, 87036, Italy
[6]Department of Biological, Geological and Environmental Sciences, University of Bologna, Bologna, 40126, Italy

CRediT statement: *Writing-original draft*: CM. *Writing-review & editing*: CM, CALJ, NS, SGL, FM, DC. *Visualization*: CM, DC. *Formal analysis*: CM, CALJ, NS, SGL, DC. *Investigation*: CM, CALJ, NS, SGL, DC. *Methodology*: CM, FM, DC.

*Corresponding author: Candela Martínez, candela.martinez@ccia.uned.es

Abstract

Normal fault growth models are largely based on the geometric relationship between fault displacement and length, and the seismically imaged record of accommodation development contained within syn-rift strata. Here, we infer variations in the style of normal fault growth across poorly exposed faulted margins through sedimentological and stratigraphic analysis of the syn-rift deposits. We analyze the along-strike variability of normal-fault controlled deltaic systems to infer the evolution of the basin-margin fault system. The geometry and displacement patterns are constrained. The Crati Basin (southern Italy) contains Pleistocene syn-rift deposits exposed in the hanging wall of a c. 45 km-long normal fault system. We show that during the early extensional phase, shelf-type deltas were deposited along the entire strike length of the fault system, suggestive of relatively shallow-water deposits and early establishment of the fault. The later extensional phase resulted in the deposition of Gilbert-type deltas at the center and towards the northern end of the fault system, whereas shelf-type deltas persisted near the southern tip of the system. This stratigraphic evolution records the transition to a period when the fault system growth was characterized by displacement accumulation rather than lengthening. We show that the detailed sedimentological and stratigraphic analysis of exposed ancient deltaic systems can be used to discriminate between models for normal fault growth. Furthermore, displacement and accommodation variations along normal faults control the styles and depositional architecture of deltaic systems in extensional settings. Results have important implications for interpreting basin-margin architectures and for predicting stratigraphic patterns in active extensional settings.

Research Article

Executive Editor
Murray Gingras

Associate Editor
Ludvig Löwemark

Reviewers
Xin Shan
Anonymous reviewer

Production Manager
Jarred Lloyd

Copy Editor
Georgina Virgo

Received: 2025-04-08
Accepted: 2025-10-07
Published: 2026-01-19

Keywords
fault-controlled deposits
deltaic systems
normal fault systems
growth
sedimentology
stratigraphic architecture

Plain language summary

Normal fault growth is affected by the amount of fault displacement and how this displacement is distributed along the length of the fault. Along-strike displacement controls the way in which space is created to allow the deposition of sediments, leading to the development of normal fault-controlled deposits. These deposit characteristics (e.g., thickness variation, stratigraphic and depositional architecture, facies distribution) are used to constrain phases of fault activity and fault growth models. This study analyzes fault-controlled deltaic systems related to a poorly exposed faulted margin. We aim to infer the evolution of the faulted margin based on the stratigraphic and along-strike variability of normal fault-controlled deposits. We show that the analysis of stratigraphic and architectural variability in normal-fault deltaic systems provides important information about the spatial and temporal evolution of normal fault systems. This approach is particularly useful along fault systems that are poorly exposed.

Riassunto

I modelli di crescita delle faglie normali si basano in gran parte sulla relazione geometrica tra rigetto e lunghezza della faglia, e sulla geometria dei depositi di sin-rift in risposta alla creazione di spazio. In questo lavoro, ricostruiamo variazioni nello stile di crescita delle faglie normali in margini poco esposti in affioramento attraverso l'analisi sedimentologica e stratigrafica dei depositi di sin-rift. Analizziamo la variabilità lungo la faglia dei sistemi deltizi per comprendere l'evoluzione del sistema di faglie. Il Bacino del Crati (Arco Calabro) contiene depositi di sin-rift pleistoceni esposti lungo il margine di un sistema di faglie normali lungo c. 45 km. In questo lavoro osserviamo che durante la fase estensionale iniziale, delta di tipo shelf si sono depositati, lungo l'intera lunghezza della faglia, in acque relativamente poco profonde. La successiva fase estensionale ha portato alla deposizione di delta di tipo Gilbert al centro e verso l'estremità settentrionale del sistema, mentre la deposizione di delta di tipo shelf è continuata in prossimità dell'estremità meridionale. Questa evoluzione stratigrafica registra la transizione ad un periodo in cui la crescita del sistema di faglie era caratterizzata da alti tassi di rigetto verticale. In questo lavoro, dimostriamo che l'analisi sedimentologica e stratigrafica dettagliata di antichi sistemi deltizi esposti può essere utilizzata per comprendere i modelli di crescita di faglie normali. Inoltre, in contesti estensionali le variazioni di rigetto e accomodamento lungo faglie normali controllano lo stile e l'architettura deposizionale dei sistemi deltizi.

1 Introduction

Many studies have used thickness variations, stratigraphic architecture, and facies distribution within syn-rift strata to constrain phases of fault activity (e.g., Bell et al., 2009; Gawthorpe, Jackson, et al., 2003; Henstra et al., 2016; Martínez et al., 2024; Young et al., 2003), and growth models for normal faults (e.g., Bell et al., 2009; Gawthorpe, Jackson, et al., 2003; Gupta et al., 1999; Jackson et al., 2002, 2017; Young et al., 2002). Fault-controlled deltaic systems may develop during rifting (Barrett et al., 2019; Colella, 1988; Ford et al., 2013), and their facies types and stacking patterns, for example, can provide a record of spatial and temporal variations in fault total displacement and slip rates, and overall patterns of syn-rift subsidence (e.g., Backert et al., 2010; Dorsey et al., 1995; Ford et al., 2013; Gawthorpe, Hardy, et al., 2003; Hardy & Gawthorpe, 1998).

The most used classifications for deltaic systems are based on the dominant delta front regime (i.e., wave, tide, river; Ainsworth et al., 2011; Galloway, 1975; Hampson & Howell, 2017) or their tectono-geomorphic setting (e.g., shelf-, slope-, and Gilbert-type deltas; Ethridge & Wescott, 1984). In this study, we analyzed fault-controlled deltaic systems using the BSG (Base-of-scarp, Shoal-water/shelf-type, Gilbert-type deltas) ternary diagram proposed by Chiarella et al. (2021). This diagram describes three end-members of base-of-scarp (B) deltas, shoal-water/shelf-type (S) deltas and Gilbert-type (G) deltas. The classification proposed by Chiarella et al. (2021) is based on the morphological stability of the deposits and throw of the controlling fault. These fault-controlled systems (B, S, and G) are thought to evolve from unsteady (B) to steady-state (S and G) conditions (*sensu* Chiarella et al., 2021; Prior & Bornhold, 1988). This change can be recorded by the transition from stratigraphically disorganized, texturally immature base-of-scarp (B) to more organized, texturally mature shelf- or Gilbert-type deltas (S or G; Chiarella et al.,

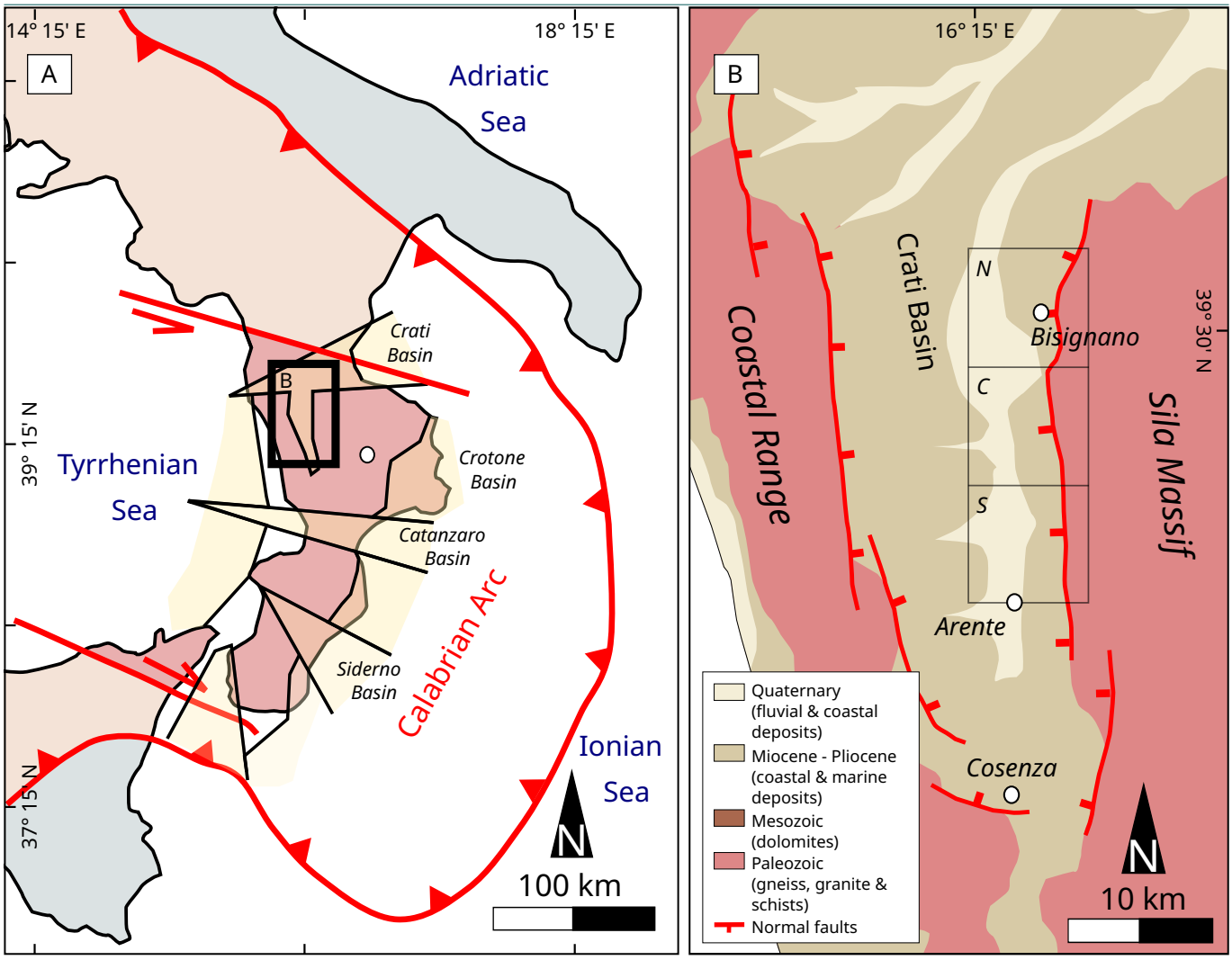

Figure 1 – **(A)** Schematic map displaying Plio-Pleistocene block-segmentation of the Calabrian Arc. Major geological entities are highlighted in light yellow (e.g., Crati, Crotone, Catanzaro, Siderno basins). Modified after Chiarella et al. (2021). **(B)** Schematic geological map of the Crati Basin. Studied sectors (i.e., northern, central, and southern) are highlighted, as well as the faulted areas that serve as the eastern and western margins of the Crati Basin. Modified after Colella (1988).

2021, Figure 2). Shelf- and Gilbert-type deltas differ in their architecture: Gilbert-type deltas display a tripartite architecture (i.e., topset, foreset, bottomset), whereas shelf-type deltas are characterized by a simpler, subhorizontal, and laterally continuous strata pattern and a lack of any evident clinoform stratal geometry. The development of either system under steady-state conditions is controlled by the amount of relief across the basin-bounding fault, or more specifically, accommodation generated in the hanging wall. Low accommodation favors the development of low-relief and gently inclined shelf-type deltas, and high accommodation produces high-relief, tripartite Gilbert-type systems.

Our study area is located in the Crati Basin, southern Italy (Figure 1A), which is bounded to the west and east by N–S-striking normal faults (Figure 1B) that have been active since the Early–Middle Pleistocene (Robustelli & Muto, 2017; Spina et al., 2011). This study analyzes Pleistocene deposits that accumulated on the eastern margin of the Crati Basin (Figure 1), which has been characterized by an increase in displacement rate across the central sector since the Middle Pleistocene (Spina et al., 2011).

Our objective is to determine the stratigraphical and architectural variability of Pleistocene fault-controlled shelf- and Gilbert-type deltas (Colella et al., 1987; Colella, 1988; Fabbricatore et al., 2014), and to use these to infer the relative temporal and spatial evolution of the faulted margin. The analyzed depositional systems accumulated during the same phase of basin evolution (i.e., Middle to Late Pleistocene) based on biostratigraphic data from Colella et al. (1987) and Fabbricatore (2011), and in response to similar sedimentation rates (Fabbricatore et al., 2014; Young & Colella, 1988).

2 Material and Methods

The study area was divided into three sectors (i.e., southern, central, and northern; Figure 1B), within which we analyzed thirty-nine exposed sections (Supplementary Material 1). The sedimentary analysis comprised: (i) the description of depositional architecture, with emphasis on external geometry, layer architecture, and arrangement of the sedimentary structures; (ii) sedimentary logging; and (iii) facies analysis, including descriptions of sedimentary structures, textures, grading, color, etc. Mudstone-dominated prodelta deposits have not been investigated in detail because they are not particularly exposed and mostly preserved below present-day fluvial deposits of the Crati River. Moreover, these deposits are not diagnostic of delta architecture, nor are they indicative of the evolution of the bounding fault. Due to the lack of continuity between outcrops over large distances, we used their location (i.e., Geographical Coordinate System) and altitude (i.e., elevation above sea level) to relate their stratigraphic positions and to correlate sedimentary logs. We consider this approach valid because regional post-depositional uplift across central Calabria was broadly uniform over the last 3 million years with no internal deformation of the basin fill (Quye-Sawyer et al., 2021).

3 Geological Background

The Crati Basin forms part of the northern sector of the Calabrian Arc, a continental fragment thrust onto Mesozoic and Tertiary sediments (Butler et al., 2004; Figure 1A) during the collision of the African (Adriatic plate) and Eurasian plates (Patacca et al., 1990). This process formed the Tyrrhenian-Ionian subduction system, with the Ionian oceanic lithosphere subducting under the Eurasian plate (Guarnieri, 2006). Subduction led to back-arc extension, the opening of the Tyrrhenian Basin (Magni et al., 2014), and the rapid SE migration and fragmentation of the Calabrian Arc into NW-trending, internally sheared blocks (e.g., Crotone, Catanzaro, Siderno Basins). The Calabrian Arc is separated from the adjacent northern Apennines and southern Maghrebide segments (Bonardi et al., 2005; Spina et al., 2011) by two major NW–SE-striking shear zones (Figure 1A): the sinistral Pollino Line to the north (Busquet & Gueremy, 1969; Turco et al., 1990; Wortel & Spakman, 1993) and the dextral Taormina Line to the south (Amodio Morelli et al., 1976; Argnani et al., 2009).

This study focuses on the Pleistocene syn-rift deposits that accumulated along the eastern margin of the Crati Basin (Figure 1B). The basin is located in the back-arc domain of the Tyrrhenian-Ionian subduction system, initially forming in the Early Pleistocene (Corradino et al., 2020; Monaco & Tortorici, 2000; Scandone, 1979). The Crati Basin is an L-shaped basin (Figure 1B), bound to the north and south by long-lived, regional, NW–SE-striking, left-lateral strike-slip faults, and to the east and west by an array of N–S-striking normal faults (Spina et al., 2009; Tansi et al., 2007; Figure 1). The sedimentary infill of the Crati Basin comprises an Upper Miocene sedimentary sequence, overlain by Pliocene to Holocene clastic marine and fluvial deposits (Colella et al., 1987). Lanzafame & Tortorici (1981) divide the stratigraphic succession into two sequences. The lower sequence, recognized only in the western portion of the basin, comprises Upper Miocene–Lower Pliocene conglomerates and sandstones that grade upwards into silty claystone and unconformably overlie the Paleozoic and Mesozoic crystalline-metamorphic basement thrust belt. The upper sequence comprises Pleistocene coarse-grained deltaic and shoreline deposits, which form the focus of this study (Carobene & Damiani, 1985; Colella et al., 1987; Colella, 1988). These deposits accumulated unconformably on Upper Miocene–Lower Pliocene strata in the western side of the basin and on crystalline-metamorphic basement in the eastern side. The lateral variability in substrate type coincided with a shift in the locus of basin subsidence, which resulted in a diachronous transgression of the overlying units (Burton, 1971; Lanzafame & Tortorici, 1981; Lanzafame & Zuffa, 1976). Lastly, Middle Pleistocene alluvial and fluvial conglomerates overlay the marine Pleistocene sequences, which were deposited in response to a major uplift of the Calabrian Arc (Fabbricatore et al., 2014).

4 Results: Syn-rift Fault-controlled Deposits

The Pleistocene syn-rift succession that accumulated along the eastern margin of the Crati Basin was mainly sourced from the uplifted footwalls of the Sila Massif (Figure 1B). Sediments were deposited in a relatively shallow-marine environment and prograded westward (i.e., away from the basin-bounding fault; Colella et al., 1987; Colella, 1988; Fabbricatore et al., 2014). Facies analysis performed in the Bisignano (Colella et al., 1987; Colella, 1988) and Arente areas (Fabbricatore et al., 2014; Figure 1B), which correspond to the northern

and southernmost portions of our study area (Figure 1), was used to constrain and support the interpretation of the depositional processes (Table 1).

4.1 Facies Description and Interpretation

The integration of published data and original observations allowed us to define eight main sedimentary facies (Facies A–H, Table 1). Facies descriptions and associations, and their depositional characteristics allowed us to determine the location, size, distribution, and along-strike variability of proximal gravel (facies A–E) to distal sand-dominated deposits (facies F–H; Table 1 and Figure 2). The identified facies are similar to those previously described (e.g., Colella et al., 1987; Colella, 1988; Fabbricatore et al., 2014) and are referred to as deltaic systems. Our study emphasizes the importance of considering variability (i.e., temporal and along-strike) in the sedimentology and stratigraphic architecture of fault-controlled deltaic deposits, as similarities between depositional processes and resulting facies may be found within shelf- and Gilbert-type deltas. However, the development of gently inclined versus steeply inclined sandstone-dominated deposits (Facies F; Table 1) is used to distinguish between shelf- *versus* Gilbert-type deltas.

4.1.1 Gravel-dominated facies

Facies A consists of structureless, poorly sorted, sub-rounded to rounded pebble to boulder (up to c. 90 cm) clast-supported conglomerate, with clasts a-axis (i.e., clast longest axis) generally oriented E–W (Table 1). Clasts are organized into continuous > 1 m thick beds and interpreted to represent debrites that resulted from rapid deposition from highly concentrated, cohesionless debris flows (Gobo et al., 2014; Nemec & Steel, 1988).

Facies B is composed of poorly sorted, angular to sub-angular pebble to cobble (up to c. 7 cm) clast-supported breccia (Table 1), organized in tabular beds (< 20 cm thick). This facies is interpreted to record deposition from non-cohesive debris flows (Haughton et al., 2009; Nemec, 1990).

Facies C consists of moderately sorted, rounded pebble to boulder (up to c. 30 cm), clast-supported conglomerate (Table 1), organized into tabular, thin, continuous beds (< 20 cm thick). These deposits are generally found above Facies D (Figure 2Av) and are interpreted to have been accumulated in relation to rapid clast dispersion occurring within cohesionless debris flows (Gobo et al., 2014; Nemec & Steel, 1988).

Facies D is represented by lenticular bodies of cross-bedded, normally graded, moderately sorted, sub-rounded pebble to cobble (maximum c. 14 cm; Table 1), clast-supported conglomerate, with clasts a-axis generally oriented E–W. Clasts are arranged into > 1 m thick beds that pinch-out laterally and are defined by a concave top, and typically capped by Facies C (Figure 2Av). These deposits are interpreted to record deposition from non-cohesive turbulent flows (Fabbricatore et al., 2014; Haughton et al., 2009) or sediment reworking related to unidirectional flows.

Facies E consists of vertically stacked, lenticular bodies with a convex base, and comprise trough cross-bedded, normally-graded (Figure 2Bii), moderately sorted, sub-rounded to rounded pebble to boulder (maximum c. 70 cm; Table 1), matrix- and clast-supported conglomerate. Where present, the matrix consists of coarse-grained sands. This facies is interpreted to have been accumulated in response to sediment transportation within channels (Fabbricatore et al., 2014; Longhitano, 2008).

4.1.2 Sand-dominated facies

Facies F is composed of structureless to normally graded sandstone and pebbly conglomerate, organized into tabular beds (30 to 200 cm thick; Table 1). Based on the depositional configuration, this facies is divided into two sub-facies. Sub-facies F1 consists of gently inclined tabular beds (30 to 200 cm thick; Figure 2Biii–iv), whereas sub-facies F2 form 30 to 130 cm thick units that define relatively large-scale (up to 20 m tall), basinward-dipping foresets (Figure 2Bii–iii). Both sub-facies are characterized by an overall westward-fining trend (from granules to fine sands) and are interpreted to record tractional deposition from highly concentrated, sandy debris flows (Haughton et al., 2009; Surlyk, 1978). Bioclastic fragments referable to marine bivalves are present.

Facies G is defined by hummocky cross-stratified, moderately sorted, sub-rounded, coarse-grained sandstones, organized into continuous 20 to 200 cm beds (Table 1). This facies is interpreted to have been accumulated in relation to high-energy storm events (Dumas & Arnott, 2006). Bivalves organized in shell-rich layers are distributed within the deposits and are

	Facies	Outcrop Example	Description & Interpretation
Gravel-dominated	Facies A	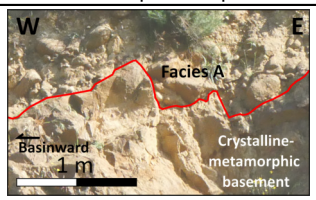	**Description** Structureless beds (> 100 cm thick) of clast-supported conglomerate. Poorly sorted, sub-angular to rounded, pebble to boulder clasts (6 to 90 cm). Clasts longest axis generally oriented E–W. **Interpretation** Rapid, highly concentrated, non-cohesive debris flows.
	Facies B	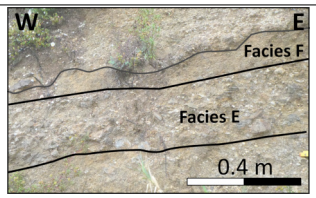	**Description** Crude tabular beds (< 20 cm thick) of clast-supported breccia. Poorly sorted, angular to sub-angular, pebble to cobble clasts (0.4 to 7 cm). **Interpretation** Laminar flow related to non-cohesive debris flows.
	Facies C	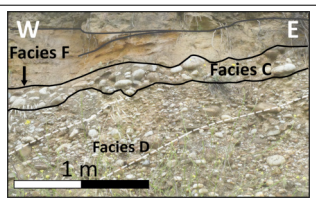	**Description** Thin continuous beds (< 20 cm thick) of clast-supported conglomerate, generally overlying Facies D. Moderately sorted, rounded, cobble to boulder clasts (7 to 30 cm). Clasts longest axis oriented E–W. **Interpretation** Rapid clast dispersion related to a non-cohesive debris flows.
	Facies D	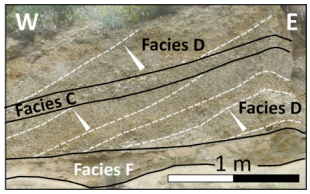	**Description** Lenticular bodies (< 100 cm thick) of clast-supported conglomerate that pinch out laterally with a concave top. Cross-bedded, normally graded, moderately sorted, pebble to cobble clasts (0.5 to 14 cm). Clasts longest axis oriented E–W. **Interpretation** Non-cohesive turbulent flow or tractional transportation related to unidirectional flows.
	Facies E	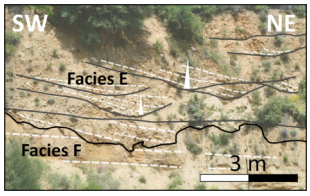	**Description** Vertically stacked lenticular bodies (> 100 cm thick) of matrix- and clast-supported conglomerate with a convex base, sandy matrix. Through cross-bedded, normally graded, moderately sorted, sub-rounded to rounded, pebble to cobble clasts (4 to 70 cm). **Interpretation** Sediment transportation through traction along channelised paths (i.e., channel fill-deposits).
Sand-dominated	Facies F	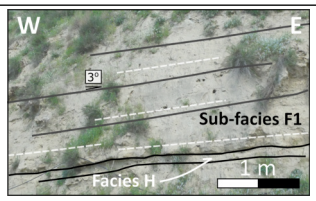 Sub-facies 1 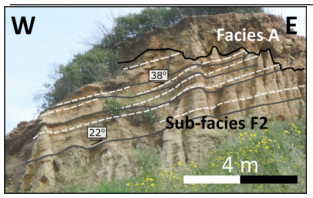 Sub-facies 2	**Description** Vertically stacked tabular beds (<200 cm thick) of sandstone and pebbly conglomerate. Structureless to normally graded, moderately sorted, sub-angular grains. Pebble clasts and carbonate bioclasts are dispersed or scattered into apparently non-continuous thin layers. Overall westward (basinward) fining trend. Based on the depositional configuration of the beds distinguished between Sub-facies F1 (sub-horizontal) and F2 (inclined 12–35 degrees). **Interpretation** Tractional, rapid, highly concentrated sandy flows.
	Facies G	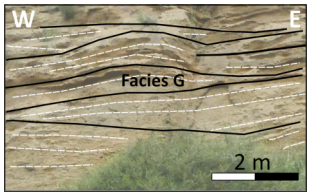	**Description** Continuous beds of variable thickness (20 to 200 cm) coarse-grained sandstone interbedded with Facies F. Hummocky cross-stratification of moderately sorted sandstone. **Interpretation** Deposition related to high-energy events (i.e., storm) resulting in oscillatory flows.
	Facies H	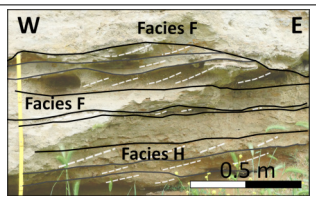	**Description** Continuous beds (< 15 cm thick) of coarse-grained sandstone to gravel (0.07 to 0.3 cm) with an asymmetrical wavy top. Cross-lamination of moderately sorted, sub-rounded sandstone. **Interpretation** Deposition related to a unidirectional current, resulting in the tractional transportation of sand grains and resulting in the migration of subaqueous bars.

Table 1 – Summary of the main facies recognized in the eastern margin of the Crati Basin.

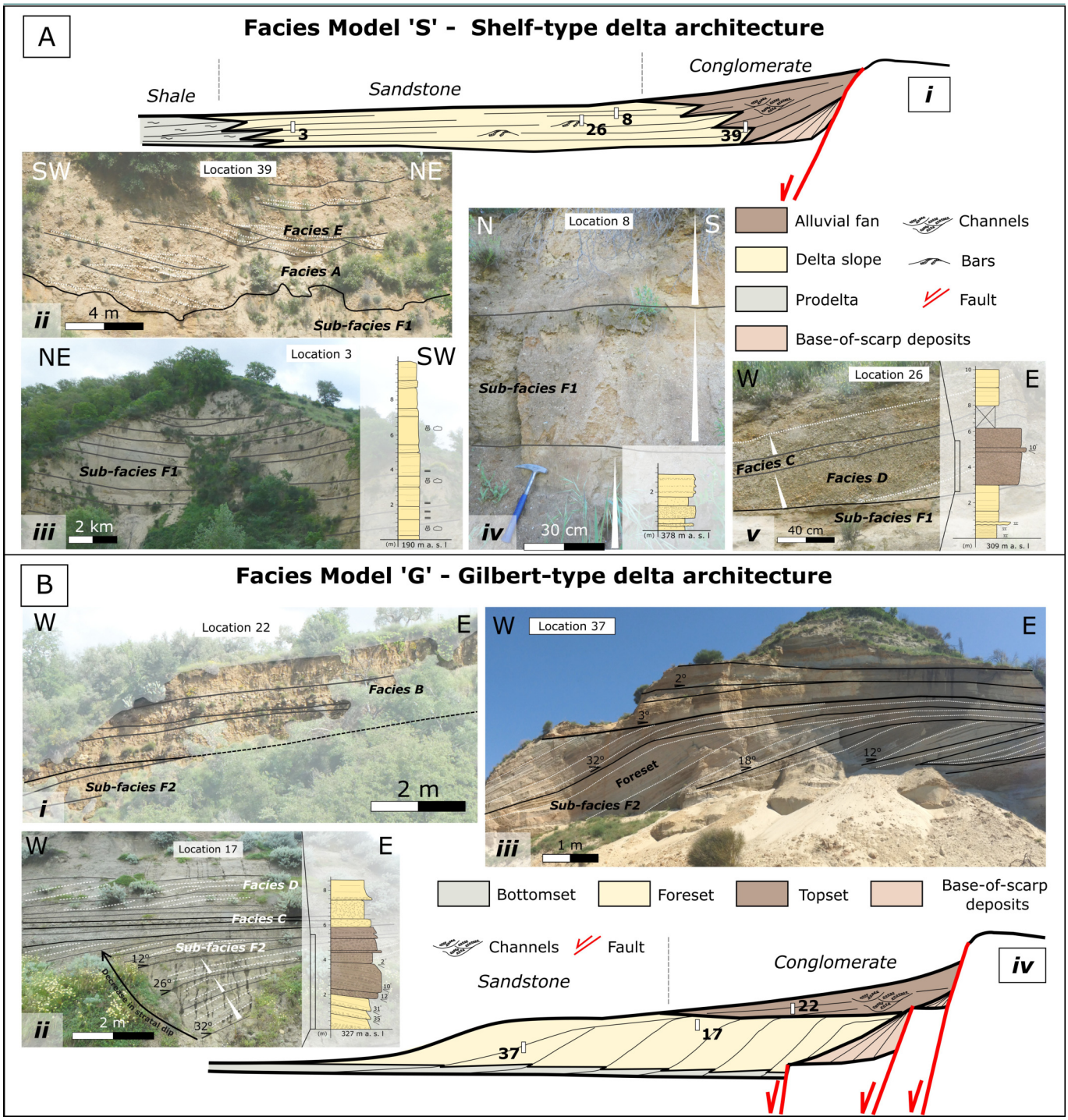

Figure 2 – **(A)** Idealized depositional model, architecture, and facies of shelf-type deltas (i–v). This type of system is characterized by the dominance of gently inclined tabular beds of deposits of sub-facies F1. **(B)** Idealized depositional model, architecture, and facies of Gilbert-type deltas (i–iv). This system is characterized by foresets mainly composed of sub-facies F2. Displayed numbers (i.e., 2Ai and 2Biv) indicate the stratigraphic position and locations of the studied areas and measured logs. Cgl = conglomerate; Sst = sandstone; Sh = shale/mudstone.

interpreted to have potentially resulted from high-energy (storm or tsunami) events.

Facies H consists of cross-laminated, moderately sorted, sub-rounded coarse-grained sandstones, organized into up to 15 cm thick continuous beds (Table 1), and characterized by an asymmetrical, wavy top. Paleocurrent measurements indicate transport to the west (Table 1). These deposits are interpreted to record deposition of subaqueous bars formed under unidirectional currents and reworked by fair-weather waves (Fabbricatore et al., 2014; Rasmussen, 2000).

4.2 Facies Associations

The detailed logging of deposits revealed eight main component facies (Table 1), which form two main facies

associations—referable to shelf-type and Gilbert-type delta facies models.

Facies A–E, F1, G, and H are genetically related. For example, conglomeratic (Facies A, C–E) and breccia (Facies B) deposits dominate proximal areas immediately adjacent to the basin-bounding faults, forming an alluvial fan, and showing a fining-basinward trend resulting in gently inclined, delta slope sandstone-dominated facies (Facies F–H; Figure 2Bii). Gently inclined sandstone and conglomerate deposits of the sub-facies F1 dominate and extend basinward for at least c. 1.27 km, intercalated with deposits of Facies E, G, and H (Figure 2Av; Table 1). In this system, we interpret this facies association as representative of shelf-type delta deposits (Figure 2A; facies model 'S' *sensu* Chiarella et al., 2021). The interpretation is supported by the proximal accumulation of alluvial fan conglomeratic deposits (Facies A), passing basinward into gently inclined delta slope deposits (sub-facies F1; Figure 2Biii), and the overall proximal-to-distal fining trend (Figure 2Bi and Table 1; Colella, 1988; Fabbricatore et al., 2014; Swift & Thorne, 1992).

Facies A–E and F2 are related deposits. As for the facies model 'S', conglomeratic (Facies A) and breccia (Facies B) deposits dominate in the proximal areas close to the basin-bounding fault. However, in contrast to the facies model 'S', these proximal deposits are organized into slightly inclined, basinward-dipping strata (up to 5°) overlying more steeply inclined (up to 35°), sandstone-dominated foresets of sub-facies F2 (Figure 2Bi). Deltaic foresets dip westward (Figure 2Bii–ii) into the basin for at least 1.5 km. Conglomeratic bars and channel fill deposits (Facies C–E) are found at the topset-foreset transition (i.e., delta-brink zone *sensu* Gobo et al., 2014; Figure 2Bii). The upward transition from steeply inclined foresets to sub-horizontal topsets, and the overall coarsening-upward trend, suggest this facies assemblage is representative of Gilbert-type delta deposits (Figure 2B; facies model 'G' *sensu* Chiarella et al., 2021).

4.3 Architectural Variability of Deltaic Deposits

We correlated twenty-nine sedimentary logs across the three studied sectors (Figure 1B) based on analysis of facies, stratigraphic position, depositional architecture and their resulting thickness in the context of displacement and accommodation variations along the basin-bounding faults (Figure 3). Although the study area was not always walkable along-strike, biostratigraphic data collected by Colella et al. (1987) and Fabbricatore (2011) allowed us to infer that the studied deposits exposed along the eastern margin (i.e., from the Bisignano to the Arente areas; Figure 1B) are age-equivalent.

Overall, the studied succession thickens northward from 240 to 325 m, suggesting a general increase in accommodation in that direction. The distribution of the described facies and related 'S' and 'G' facies models indicate that during the earliest stage of deposition, shelf-type delta deposits developed in all three sectors (Figures 3, 4B). In contrast, during the late stage (Figure 4Bii), Gilbert-type delta deposits accumulated only across the central and northern sectors (Figure 3B–C), whereas deposition of shelf-type deltas continued in the southern sector (Figure 3A).

5 Discussion: Fault-controlled Deltaic Systems and Architectural Variability

In addition to sedimentation rate and depositional regime (e.g., waves, tides, rivers), the sedimentology and stratigraphic architecture of syn-rift depositional systems are also controlled by temporal and spatial changes in fault displacement rate and total displacement (e.g., migration of fault tip *versus* center; Chiarella et al., 2021; Gawthorpe et al., 1994; Gawthorpe & Colella, 1990; Hardy & Gawthorpe, 1998). These two variables control accommodation distribution, sediment input and *loci* of sediment accumulation along faults. Therefore, the stratigraphic and architectural analysis of normal fault-controlled deposits provides critical constraints (or insights) for the growth model and evolution of a basin-margin fault system (e.g., Backert et al., 2010; Bell et al., 2009; Young et al., 2003). Nemec (1990) suggests that depositional slopes with steep subaqueous gradients develop deltas characterized by steep foresets. These deltas progressively evolve into Gilbert-type systems under high sedimentation rate conditions, with characteristic topset, foreset, and bottomset architectures.

These morphological conditions are easily created towards the center zone of normal faults during late phases of growth, and are usually characterized by a high displacement rate. Conversely, depositional profiles having an angle of less than 5° result in the development of gently inclined beds, characteristic of shelf-type deltas (Ethridge & Wescott, 1984).

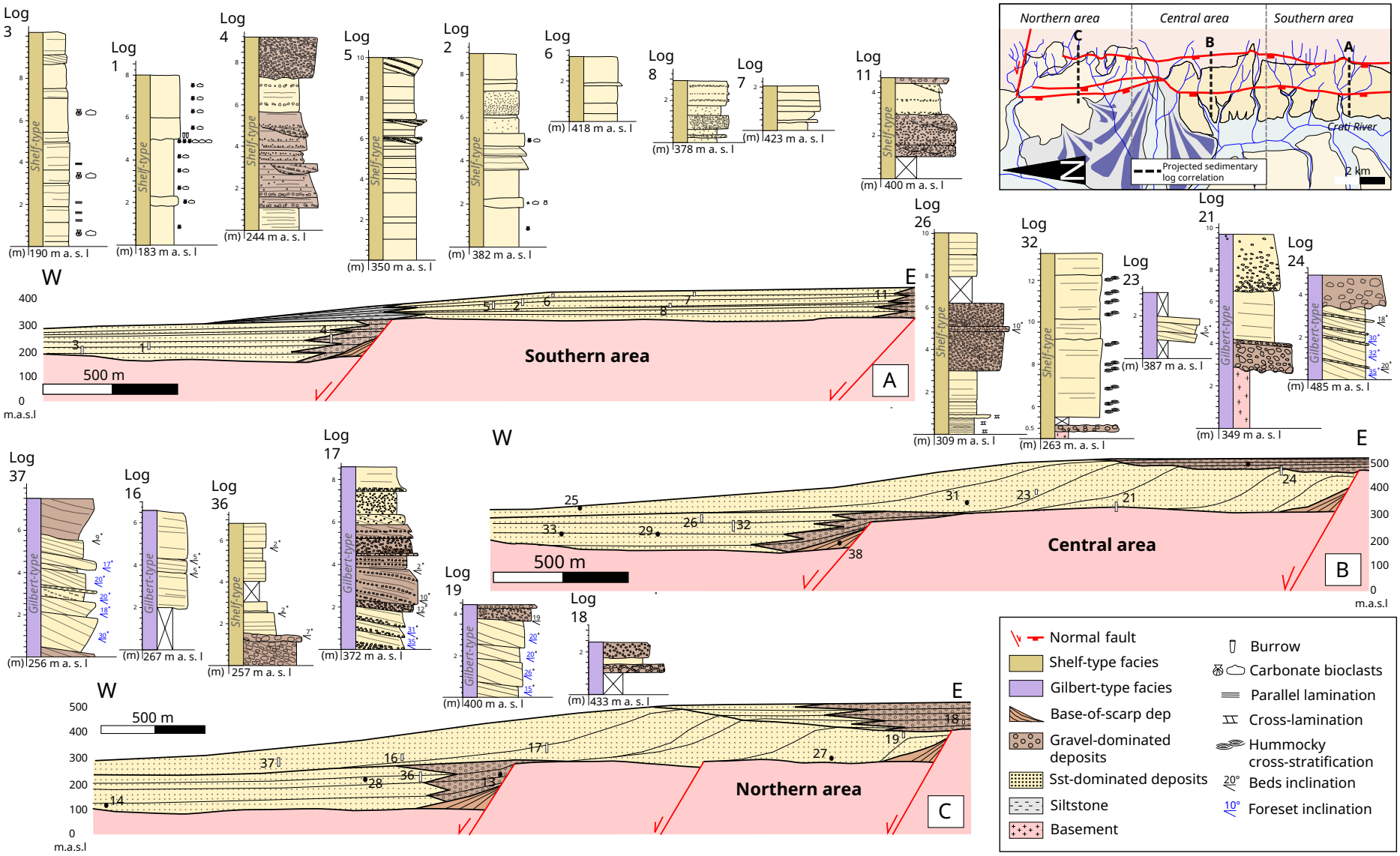

Figure 3 – Reconstruction of the Pleistocene deltaic systems accumulated along the three studied sectors based on log correlation. The logs were selected based on the area (points of interest) and the quality of the data collected. **(A)** Southern sector deposits organized into vertically stacked shelf-type deltas. **(B)** Central and **(C)** northern sectors deposits organized into shelf-type deltas, overlain by Gilbert-type deltas. Displayed numbers along the deltaic systems reconstructions indicate the stratigraphic position and locations of the displayed measured logs. The left bars in the sedimentary logs indicate the interpreted facies model (i.e., yellow for shelf-type delta 'S' and purple for Gilbert-type delta 'G' deposits). Note: the terms shelf-type and Gilbert-type within the sedimentary logs refer to shelf- and Gilbert-type delta deposits.

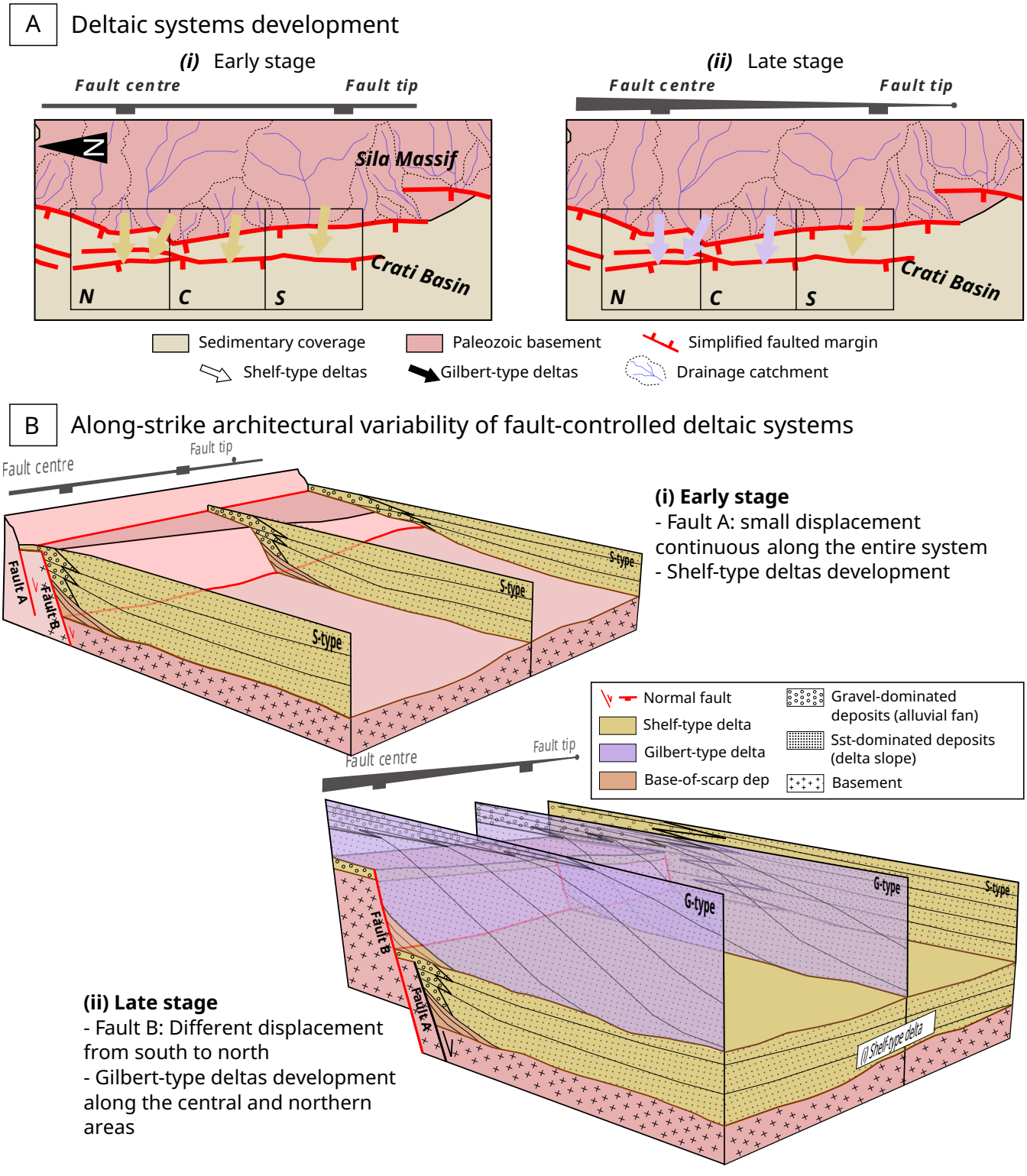

Figure 4 – **(A)** Temporal development of deltaic systems, displayed along a simplified representation of the faulted area that serves as the eastern margin of the Crati Basin (N –northern; C –central; S –southern). **Ai** Early stage: initiation of margin growth and development of shelf-type deltas, and **Aii** late stage: syn-sedimentary growth of the margin and Gilbert- and shelf-type deltas development. Modified from Massari & Colella (1988). **(B)** Along-strike architectural variability of fault-controlled deltaic systems based on the inferred evolution of the faulted margin, considering fault displacement and accommodation creation along-strike – (i) early stage and (ii) late stage.

Considering fault displacement variability, Chiarella et al. (2021) propose that in fault-controlled systems, after an embryonic phase characterized by unsteady base-of-scarp deposits, limited vertical displacement produces limited accommodation, leading to the deposition of gently inclined beds within shelf-type deltaic systems. Conversely, faults with large vertical displacement lead to high accommodation, creating the conditions for the development of the tripartite architecture (i.e., topset, foreset, bottomset) and the progradation of Gilbert-type deltaic systems. These changes in the architecture geometry and depositional style (i.e., shelf- versus Gilbert-type deltas) are controlled by the evolution of the basin-margin fault system. We argue that deltaic system variability can be used to infer normal fault system growth models, and evolution and variations in displacement and accommodation along faulted margins, considering fault displacement and accommodation are created along-strike.

Our results indicate that the Pleistocene deltaic succession exposed along the eastern margin of the Crati Basin is characterized by an overall northward increase in thickness, interpreted to reflect higher displacement and accommodation. Moreover, our sedimentological results show the development of vertically stacked shelf-type deltas along strike, and the vertical transition and lateral evolution from shelf- to Gilbert-type deltas (Figures3 and 4B). We infer that the evolution of the fault system controlling the eastern margin of the Crati Basin (Figure 4A) was characterized by an early stage of rifting with faults accruing limited displacement. During this early stage (Figure 4Bi), low displacement and accommodation, and continuous deposition promoted the development of vertically stacked shelf-type deltas along strike (Figure 3). We also determine that the fault system grew in accordance with a constant-length growth model (*sensu* Childs et al., 2017; Jackson et al., 2017) due to the development of shelf-type deltas along the entire length of the fault (i.e., Fault B in Figure 4Ai and Bi).

The following stage of margin evolution (i.e., late stage; Figure 4Aii and Bii) resulted in the vertical transition and lateral evolution from shelf- to Gilbert-type deltas (Figure 4Bii) along the central and northern sectors. The stratigraphic relationships between the early- and late-stage systems and the most landward location of the latter systems in correspondence with Fault A (Figures 3 and 4Bii) suggest that the late stage of the margin evolution occurred after a relative sea-level rise, resulting in the shift of depositional systems towards the east (landwards). We infer that higher displacement and accommodation in the central and northern portion of the faulted margin promoted the development of a more complex tripartite architecture (i.e., topset, foreset, bottomset), distinctive of Gilbert-type deltas (Figures 3B and C, and 4Bii) on top of shelf-type systems (Figure 4Aii and Bii). Low displacement rates continued to occur along the southern tip of the fault (i.e., southern sector), producing the vertical stacking of shelf-type deltas (Figures 3A and 4Bii). Accordingly, the stratigraphic evolution of the system recorded a change to a period (i.e., late stage) when the fault system growth was defined by displacement accumulation rather than lengthening. This pattern is comparable to what was documented by Jackson et al. (2017) along Fault 2 in the Gulf of Suez Rift (Egypt) and Fault 4 in the Santos Basin (offshore SE Brazil). The along-strike evolution from shelf- to Gilbert-type deltas documented in this study along a fault-controlled system in the Crati Basin is also observed in subsurface data (e.g., North Sea, Norwegian Continental Shelf, Northern Carnarvon Basin). An example from the hanging wall fill of the Rankin Fault System in the Dampier Sub-basin (Northern Carnarvon Basin, Fortuna 3D seismic survey; Martínez et al., 2024) is reported in Figure 5. Here, parallel seismic lines acquired along the fault evolution document two different depositional architectures referable to Gilbert- (Figure 5B) and shelf-type (Figure 5C) systems that developed along-strike.

6 Conclusions

Our results suggest that the analysis of syn-rift strata provides important information on the spatio-temporal evolution of normal fault systems and related depositional architecture (external geometry, layer architecture, and the arrangement of sedimentary structures), which are diagnostic for evaluating along-strike fault displacement rate changes. The main conclusions of this research are:

- Across the faulted margin, early phase rifting resulted in the accumulation of shelf-type deltas along-strike, in response to the development of low displacement faults that grew in accordance with a constant-length growth model.

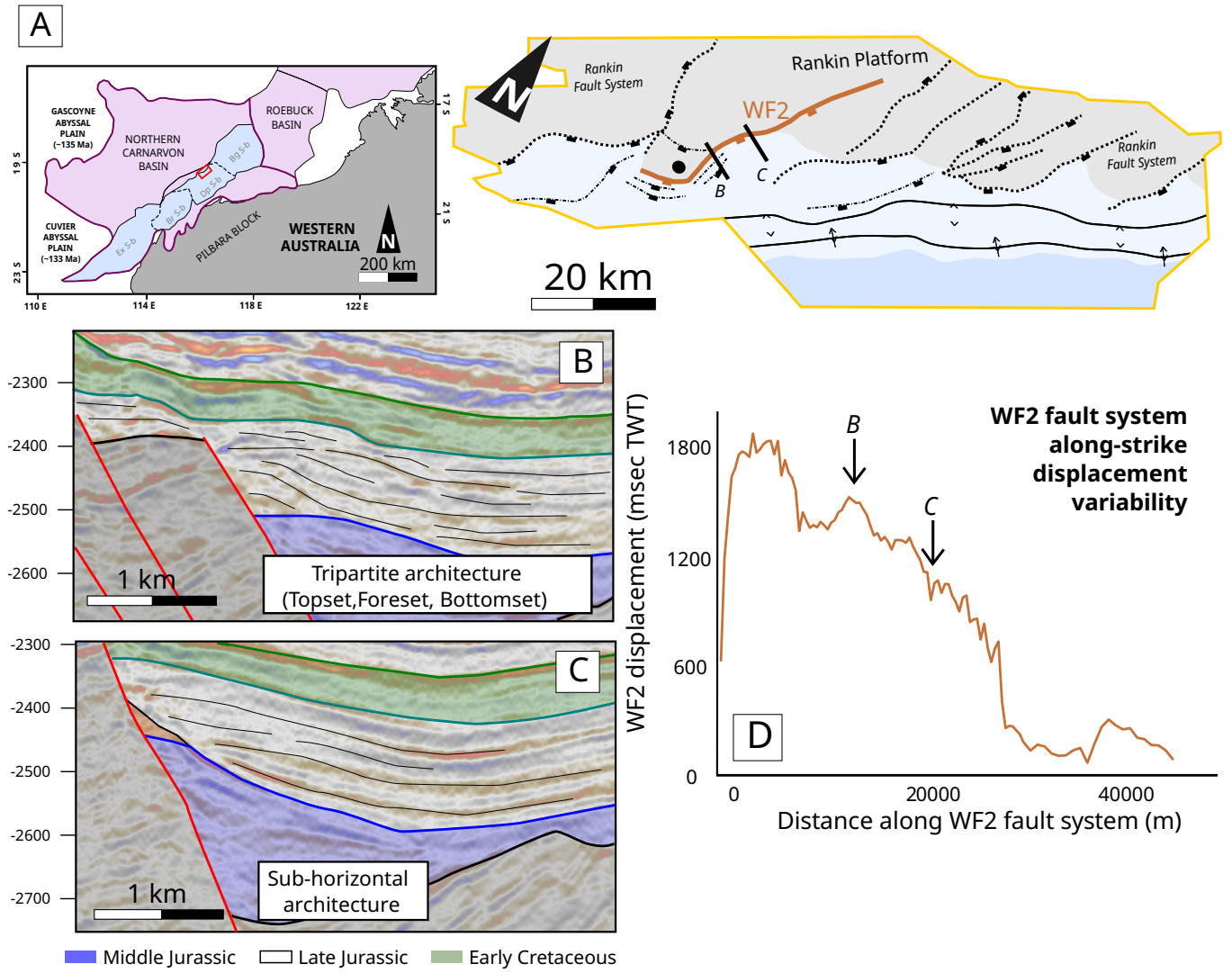

Figure 5 – **(A)** Map of the Westralian Superbasin and a schematic structural map of the western margin of the Dampier Sub-basin (Rankin Fault System), imaged in the Fortuna Seismic Survey (red rectangle in the regional map). WF2 fault system is labelled. **(B–C)** Hanging wall stratigraphic succession related to WF2 fault system. The depositional architecture of the Late Jurassic package is highlighted, showing a set of vertically-stacked depositional systems. Modified after Martínez et al. (2024). **(B)** Depositional system defined by a tripartite architecture (i.e., topset, foreset, bottomset), with basinward prograding inclined reflections, referable to a Gilbert-type deltaic system. **(C)** Depositional system defined by sub-horizontal continuous reflections referable to a shelf-type deltaic system. The chaotic reflectors forming a wedge attached to the fault are interpreted as base-of-scarp deposits (*sensu* Chiarella et al., 2021). **(D)** WF2 fault system along-strike accumulated displacement. The fault throw recorded in **(B)** and **(C)** is indicated by black arrows.

- The vertical transition and lateral evolution from shelf- to Gilbert-type deltas along the central and northern sectors record higher displacement and accommodation. Deposition of shelf-type deltas continued in the southern sector, forming a vertically-stacked arrangement, which suggests low displacement rates along that sector. Therefore, the late stage of stratigraphic evolution indicates that the fault system growth was defined by displacement accumulation rather than lengthening.
- The stratigraphic relationships between the early and late-stage systems indicate that the late stage of margin evolution occurred after a relative sea-level rise, producing a transgression and the shift of the coastline towards the east.
- Our study demonstrates that the temporal and along-strike stratigraphical and architectural analysis of deltaic deposits can be useful when trying to determine the evolution of structures that are poorly exposed in the field or deeply buried in the subsurface.

Our results are also useful for assessing the relationships between relatively high displacement rates at the fault center and the development of steep-faced morphologies (i.e., Gilbert-type), which

are characterized by sediment remobilization that promotes gravity-driven, mass-transport processes (debris flows). The results emphasize that syn-rift deltaic successions represent sensitive recorders of fault kinematics, and provide a valuable framework for refining models of rift-basin evolution by linking tectonic displacement patterns with basin-scale stratigraphic organization.

Acknowledgements

We thank the University of Calabria for support and guidance while performing field activities, and Ronald Steel and Rob Gawthorpe for a detailed review of an early version of the manuscript. The authors gratefully acknowledge Xin Shan and an anonymous reviewer for their constructive and detailed reviews.

Data and code availability

The location of all outcrops analyzed in this study is presented in the Supplementary material in Figure S1.

Supplementary material

Supplementary figure S1 can be found online with the article at doi:10.57035/journals/sdk.2026.e41.1927.

Conflict of interest statement

The authors declare they do not have any tangible or perceived conflicts of interest with regard to this research.

Artificial intelligence use statement

All research, analysis, writing, and editing were performed without generative AI assistance.

Funding

This project was sponsored by SVAL Energi (now DNO ASA Norway) who funded the PhD scholarship of CM in the Department of Earth Sciences at Royal Holloway University of London. Field activities were financially supported by Royal Holloway University of London and the British Sedimentological Research Group.

Citing this Research Article

To cite this paper use the following information:

Authors

Candela Martínez, Christopher A-L. Jackson, Nicola Scarselli, Sergio G. Longhitano, Francesco Muto, Domenico Chiarella

Title

Along-strike variability of fault-controlled deltaic systems (Crati Basin, southern Italy)

Short Title

Fault-controlled deltaic systems

Publishing Information

Publication: Sedimentologika
Volume: 4
Issue: 1
Year: 2026
DOI: 10.57035/journals/sdk.2026.e41.1927
Language: en

References

Ainsworth, R. B., Vakarelov, B. K., & Nanson, R. A. (2011). Dynamic spatial and temporal prediction of changes in depositional processes on clastic shorelines: Toward improved subsurface uncertainty reduction and management. *AAPG Bulletin*, *95*(2), 267–297. https://doi.org/10.1306/06301010036

Amodio Morelli, L., Bonardi, G., Colonna, V., Dietrich, D., Giunta, G., Ippolito, F., Liguori, V., Lorenzoni, S., Paglionico, A., Perrone, V., Piccarreta, G., Russo, M., Scandone, P., Zanettin Lorenzoni, E., & Zuppetta, A. (1976). L'arco Calabro-Peloritano nell'orogene appenninico Maghrebide. *Italian Journal of Geosciences*, *17*, 1–60.

Argnani, A., Brancolini, G., Bonazzi, C., Rovere, M., Accaino, F., Zgur, F., & Lodolo, E. (2009). The results of the Taormina 2006 seismic survey: Possible implications for active tectonics in the Messina Straits. *Tectonophysics*, *476*(1–2), 159–169. https://doi.org/10.1016/j.tecto.2008.10.029

Backert, N., Ford, M., & Malartre, F. (2010). Architecture and sedimentology of the Kerinitis Gilbert-type fan delta, Corinth Rift, Greece. *Sedimentology*, *57*(2), 543–586. https://doi.org/10.1111/j.1365-3091.2009.01105.x

Barrett, B. J., Collier, R. E. Ll., Hodgson, D. M., Gawthorpe, R. L., Dorrell, R. M., & Cullen, T. M. (2019). Quantifying faulting and base level controls on syn-rift sedimentation using stratigraphic architectures of coeval, adjacent Early-Middle Pleistocene fan deltas in Lake Corinth, Greece. *Basin Research*, *31*(6), 1040–1065. https://doi.org/10.1111/bre.12356

Bell, R. E., McNeill, L. C., Bull, J. M., Henstock, T. J., Collier, R. E. L., & Leeder, M. R. (2009). Fault architecture, basin structure and evolution of the Gulf of Corinth Rift, central Greece. *Basin Research*, *21*(6), 824–855. https://doi.org/10.1111/j.1365-2117.2009.00401.x

Bonardi, G., Capoa, P. D., Di Staso, A., Perrone, V., Sonnino, M., & Tramontana, M. (2005). The age of the Paludi Formation: a major constraint to the beginning of the Apulia-verging orogenic transport in the northern sector of the Calabria–Peloritani Arc. *Terra Nova*, *17*(4), 331–337. https://doi.org/10.1111/j.1365-3121.2005.00618.x

Burton, A. N. (1971). *Carta Geologica della Calabria alla scala di 1:25.000: Relazione generale*. Cassa per il Mezzogiorno, Servizio Bonifiche.

Busquet, J.-C., & Gueremy, P. (1969). Quelques phénomènes de néotectonique dans l'Apennin Calabro-Lucanien et leurs conséquences morphologiques. II. L'escarpment méridional du Pollino et son piémont. *Revue De Géographie Physique Et Géologie Dynamique*, *11*, 223–236.

Butler, R. W. H., Mazzoli, S., Corrado, S., Donatis, M. D., Bucci, D. D., Gambini, R., Naso, G., Nicolai, C., Scrocca, D., Shiner, P., & Zucconi, V. (2004). Applying Thick-skinned Tectonic Models to the

Apennine Thrust Belt of Italy—Limitations and Implications. In K. R. McClay (Ed.), *Thrust Tectonics and Hydrocarbon Systems: Vol. 82: AAPG Memoir* (pp. 647–667). American Association of Petroleum Geologists. https://doi.org/10.1306/M82813C34

Carobene, L., & Damiani, A. V. (1985). Tettonica e sedimentazione pleistocenica nella media valle del fiume Crati. Area tra il torrente Pescara ed il fiume Mucone (Calabria). *Italian Journal of Geosciences*, *104*(1), 115–127.

Chiarella, D., Capella, W., Longhitano, S. G., & Muto, F. (2021). Fault-controlled base-of-scarp deposits. *Basin Research*, *33*(2), 1056–1075. https://doi.org/10.1111/bre.12505

Childs, C., Holdsworth, R. E., Jackson, C. A.-L., Manzocchi, T., Walsh, J. J., & Yielding, G. (2017). Introduction to the geometry and growth of normal faults. *Geological Society, London, Special Publications*, *439*(1), 1–9. https://doi.org/10.1144/SP439.24

Colella, A. (1988). Pliocene-Holocene fan deltas and braid deltas in the Crati Basin, Southern Italy: a consequence of varying tectonc conditions. In W. Nemec & R. J. Steel (Eds.), *Fan Deltas: Sedimentology and Tectonic Settings* (pp. 50–74). Blackie and Son.

Colella, A., De Boer, P. L., & Nio, S. D. (1987). Sedimentology of a marine intermontane Pleistocene Gilbert-type fan-delta complex in the Crati Basin, Calabria, southern Italy. *Sedimentology*, *34*(4), 721–736. https://doi.org/10.1111/j.1365-3091.1987.tb00798.x

Corradino, M., Pepe, F., Bertotti, G., Picotti, V., Monaco, C., & Nicolich, R. (2020). 3-D Architecture and Plio-Quaternary Evolution of the Paola Basin: Insights Into the Forearc of the Tyrrhenian-Ionian Subduction System. *Tectonics*, *39*(2), e2019TC005898. https://doi.org/10.1029/2019TC005898

Dorsey, R. J., Umhoefer, P. J., & Renne, P. R. (1995). Rapid subsidence and stacked Gilbert-type fan deltas, Pliocene Loreto basin, Baja California Sur, Mexico. *Sedimentary Geology*, *98*(1–4), 181–204. https://doi.org/10.1016/0037-0738(95)00032-4

Dumas, S., & Arnott, R. W. C. (2006). Origin of hummocky and swaley cross-stratification— The controlling influence of unidirectional current strength and aggradation rate. *Geology*, *34*(12), 1073. https://doi.org/10.1130/G22930A.1

Ethridge, F. G., & Wescott, W. A. (1984). Tectonic Setting, Recognition and Hydrocarbon Reservoir Potential of Fan Deltas. In *Sedimentology of Gravels and Conglomerates: Vol. 10: AAPG Memoir* (pp. 217–335). American Association of Petroleum Geologists.

Fabbricatore, D. (2011). *Stratigarfia e analisi di facies dei depositi quaternari affioranti in destra della media Valle del Fiume Crati (Calabria Settentrionale)* [Doctoral thesis, University of Calabria]. https://hdl.handle.net/20.500.14242/145889

Fabbricatore, D., Robustelli, G., & Muto, F. (2014). Facies analysis and depositional architecture of shelf-type deltas in the Crati Basin (Calabrian Arc, south Italy). *Italian Journal of Geosciences*, *133*(1), 131–148. https://doi.org/10.3301/IJG.2013.19

Ford, M., Rohais, S., Williams, E. A., Bourlange, S., Jousselin, D., Backert, N., & Malartre, F. (2013). Tectono-sedimentary evolution of the western Corinth rift (Central Greece). *Basin Research*, *25*(1), 3–25. https://doi.org/10.1111/j.1365-2117.2012.00550.x

Galloway, W. E. (1975). Process framework for describing the morphology and stratigraphic evolution of the deltaic depositional systems. In M. L. Broussard (Ed.), *Deltas: Models for Exploration* (pp. 87–98). Houston Geological Society.

Gawthorpe, R. L., & Colella, A. (1990). Tectonic Controls on Coarse-Grained Delta Depositional Systems in Rift Basins. In A. Colella & D. B. Prior (Eds.), *Coarse-grained deltas: Vol. 10: Special Publication of the International Association of Sedimentologists* (1st ed., pp. 113–127). Wiley. https://doi.org/10.1002/9781444303858.ch6

Gawthorpe, R. L., Fraser, A. J., & Collier, R. E. L. (1994). Sequence stratigraphy in active extensional basins: implications for the interpretation of ancient basin-fills. *Marine and Petroleum Geology*, *11*(6), 642–658. https://doi.org/10.1016/0264-8172(94)90021-3

Gawthorpe, R. L., Hardy, S., & Ritchie, B. (2003). Numerical modelling of depositional sequences in half-graben rift basins. *Sedimentology*, *50*(1), 169–185. https://doi.org/10.1046/j.1365-3091.2003.00543.x

Gawthorpe, R. L., Jackson, C. A.-L., Young, M. J., Sharp, I. R., Moustafa, A. R., & Leppard, C. W. (2003). Normal fault growth, displacement localisation and the evolution of normal fault populations: the Hammam Faraun fault block, Suez rift, Egypt. *Journal of Structural Geology*, *25*(6), 883–895. https://doi.org/10.1016/S0191-8141(02)00088-3

Gobo, K., Ghinassi, M., & Nemec, W. (2014). Reciprocal Changes In Foreset To Bottomset Facies In A Gilbert-Type Delta: Response To Short-Term Changes In Base Level. *Journal of Sedimentary Research*, *84*(11), 1079–1095. https://doi.org/10.2110/jsr.2014.83

Guarnieri, P. (2006). Plio-Quaternary segmentation of the south Tyrrhenian forearc basin. *International Journal of Earth Sciences*, *95*(1), 107–118. https://doi.org/10.1007/s00531-005-0005-2

Gupta, S., Underhill, J. R., Sharp, I. R., & Gawthorpe, R. L. (1999). Role of fault interactions in controlling synrift sediment dispersal patterns: Miocene, Abu Alaqa Group, Suez Rift, Sinai, Egypt. *Basin Research*, *11*(2), 167–189. https://doi.org/10.1046/j.1365-2117.1999.00300.x

Hampson, G. J., & Howell, J. A. (2017). Sedimentologic and sequence-stratigraphic characteristics of wave-dominated deltas. *AAPG Bulletin*, *101*(4), 441–451. https://doi.org/10.1306/011817DIG17023

Hardy, S., & Gawthorpe, R. L. (1998). Effects of variations in fault slip rate on sequence stratigraphy in fan deltas: Insights from numerical modeling. *Geology*, *26*(10), 911–914. https://doi.org/10.1130/0091-7613(1998)026<0911:EOVIFS>2.3.CO;2

Haughton, P., Davis, C., McCaffrey, W., & Barker, S. (2009). Hybrid sediment gravity flow deposits – Classification, origin and significance. *Marine and Petroleum Geology*, *26*(10), 1900–1918. https://doi.org/10.1016/j.marpetgeo.2009.02.012

Henstra, G. A., Grundvåg, S.-A., Johannessen, E. P., Kristensen, T. B., Midtkandal, I., Nystuen, J. P., Rotevatn, A., Surlyk, F., Sæther, T., & Windelstad, J. (2016). Depositional processes and stratigraphic architecture within a coarse-grained rift-margin turbidite system: The Wollaston Forland Group, east Greenland. *Marine and Petroleum Geology*, *76*, 187–209. https://doi.org/10.1016/j.marpetgeo.2016.05.018

Jackson, C. A.-L., Bell, R. E., Rotevatn, A., & Tvedt, A. B. M. (2017). Techniques to determine the kinematics of synsedimentary normal faults and implications for fault growth models. *Geological Society, London, Special Publications*, *439*(1), 187–217. https://doi.org/10.1144/SP439.22

Jackson, C. A.-L., Gawthorpe, R. L., & Sharp, I. R. (2002). Growth and linkage of the East Tanka fault zone, Suez rift: structural style and syn-rift stratigraphic response. *Journal of the Geological Society*, *159*(2), 175–187. https://doi.org/10.1144/0016-764901-100

Lanzafame, G., & Tortorici, L. (1981). La tettonica recente del Fiume Crati (Calabria). *Geografia Fisica E Dinamica Quaternaria*, *4*, 11–21. https://www.gfdq.glaciologia.it/index.php/GFDQ/article/view/996

Lanzafame, G., & Zuffa, G. G. (1976). Geologia e petrografia del Foglio di Bisignano (Bacino del Crati, Calabria): Carta geologica alla scala 1:50000. *Geologica Romana*, *15*, 223–270.

Longhitano, S. G. (2008). Sedimentary facies and sequence stratigraphy of coarse-grained Gilbert-type deltas within the Pliocene thrust-top Potenza Basin (Southern Apennines, Italy). *Sedimentary Geology*, *210*(3–4), 87–110. https://doi.org/10.1016/j.sedgeo.2008.07.004

Magni, V., Faccenna, C., Hunen, J., & Funiciello, F. (2014). How collision triggers backarc extension: Insight into Mediterranean style of extension from 3-D numerical models. *Geology*, *42*(6), 511–514. https://doi.org/10.1130/G35446.1

Martínez, C., Chiarella, D., Jackson, C. A.-L., Rennie, H., & Scarselli, N. (2024). Syn-rift tectono-stratigraphic development of the Thebe-0 fault system, Exmouth Plateau, offshore NW Australia: The role of fault-scarp degradation. *Basin Research*, *36*(1), e12842. https://doi.org/10.1111/bre.12842

Massari, F., & Colella, A. (1988). Evolution and types of fan-delta systems in some major tectonic settings. In W. Nemec & R. J. Steel (Eds.), *Fan Deltas: Sedimentology and Tectonic Settings* (pp. 103–122). Blackie and Son.

Monaco, C., & Tortorici, L. (2000). Active faulting in the Calabrian arc and eastern Sicily. *Journal of Geodynamics*, *29*(3–5), 407–424. https://doi.org/10.1016/S0264-3707(99)00052-6

Nemec, W. (1990). Aspects of Sediment Movement on Steep Delta Slopes. In A. Colella & D. B. Prior (Eds.), *Coarse-Grained Deltas: Vol. 10: Special Publication of the International Association of Sedimentologists* (1st ed., pp. 29–73). Wiley. https://doi.org/10.1002/9781444303858.ch3

Nemec, W., & Steel, R. J. (Eds.). (1988). *Fan deltas: sedimentology and tectonic settings* (1st ed.). Blackie and Son Ltd.

Patacca, E., Sartori, R., & Scandone, P. (1990). Tyrrhenian basin and Apenninic arcs: Kinematic relations since the late Tortonian times. *Italian Journal of Geosciences*, *45*, 425–451.

Prior, D. B., & Bornhold, B. D. (1988). Submarine morphology and processes of fjord fan deltas and related high-gradient systems: Modern examples from British Columbia. In W. Nemec & R. J. Steel (Eds.), *Fan Deltas: Sedimentology and Tectonic Settings* (pp. 103–122). Blackie and Son.

Quye-Sawyer, J., Whittaker, A. C., Roberts, G. G., & Rood, D. H. (2021). Fault Throw and Regional Uplift Histories From Drainage Analysis: Evolution of Southern Italy. *Tectonics*, *40*(4), e2020TC006076. https://doi.org/10.1029/2020TC006076

Rasmussen, H. (2000). Nearshore and alluvial facies in the Sant Llorenç del Munt depositional system: recognition and development. *Sedimentary Geology*, *138*(1–4), 71–98. https://doi.org/10.1016/S0037-0738(00)00144-5

Robustelli, G., & Muto, F. (2017). The Crati River Basin: geomorphological and stratigraphical data for the Plio–Quaternary evolution of northern Calabria, South Apennines, Italy. *Geologica Carpathica*, *68*(1), 68–79. https://doi.org/10.1515/geoca-2017-0006

Scandone, P. (1979). Origin of the Tyrrhenian Sea and Calabrian Arc. *Italian Journal of Geosciences*, *98*(1), 27–34.

Spina, V., Tondi, E., Galli, P., & Mazzoli, S. (2009). Fault propagation in a seismic gap area (northern Calabria, Italy): Implications for seismic hazard. *Tectonophysics*, *476*(1–2), 357–369. https://doi.org/10.1016/j.tecto.2009.02.001

Spina, V., Tondi, E., & Mazzoli, S. (2011). Complex basin development in a wrench-dominated back-arc area: Tectonic evolution of the Crati Basin, Calabria, Italy. *Journal of Geodynamics*, *51*(2–3), 90–109. https://doi.org/10.1016/j.jog.2010.05.003

Surlyk, F. (1978). Submarine fan sedimentation along fault scarps on tilted fault blocks (Jurassic-Cretaceous boundary, East Greenland). *Bulletin Grønlands Geologiske Undersøgelse*, *128*, 1–108. https://doi.org/10.34194/bullggu.v128.6670

Swift, D. J. P., & Thorne, J. A. (1992). Sedimentation on Continental Margins, I: A General Model for Shelf Sedimentation. In D. J. P. Swift, G. F. Oertel, R. W. Tillman, & J. A. Thorne (Eds.), *Shelf Sand and Sandstone Bodies: Geometry, Facies and Sequence Stratigraphy: Vol. 14: Special Publication of the International Association of Sedimentologists* (1st ed., pp. 1–31). Wiley. https://doi.org/10.1002/9781444303933.ch1

Tansi, C., Muto, F., Critelli, S., & Iovine, G. (2007). Neogene-Quaternary strike-slip tectonics in the central Calabrian Arc (southern Italy). *Journal of Geodynamics*, *43*(3), 393–414. https://doi.org/10.1016/j.jog.2006.10.006

Turco, E., Maresca, R., & Cappadona, P. (1990). La tettonica plio-pleistocenica del confine calabro-lucano. *Italian Journal of Geosciences*, *45*(1), 519–529.

Wortel, M. J. R., & Spakman, W. (1993). The dynamic evolution of the Apenninic-Calabrian, Hellenic and Carpathian arcs: A unifying approach. *Terra Nova Abstract Supplement*, *5*(1), 97.

Young, M. J., & Colella, A. (1988). Calcareous nannofossils from the Crati Basin. In A. Colella (Ed.), *Fan deltas-excursion guide-book* (pp. 79–96). Università della Calabria.

Young, M. J., Gawthorpe, R. L., & Sharp, I. R. (2002). Architecture and evolution of syn-rift clastic depositional systems towards the tip of a major fault segment, Suez Rift, Egypt. *Basin Research*, *14*(1), 1–23. https://doi.org/10.1046/j.1365-2117.2002.00162.x

Young, M. J., Gawthorpe, R. L., & Sharp, I. R. (2003). Normal fault growth and early syn-rift sedimentology and sequence stratigraphy: Thal Fault, Suez Rift, Egypt. *Basin Research*, *15*(4), 479–502. https://doi.org/10.1046/j.1365-2117.2003.00216.x